Indian J. Met. Hydrol. Geophys. (1978), **29**, 1 & 2, 327-334

551·553·21 : 551·509·313 : 551·513·1 (267)

The planetary boundary layer over the Arabian Sea during the NE monsoon—A numerical study

M. LAL

Atmospheric Environment Service, Canada

ABSTRACT. This paper describes the results of numerical simulation of atmospheric boundary layer over Arabian Sea during NE-Monsoon season. A one-dimensional air-sea interaction model was used to simulate the vertical profiles of momentum, heat and moisture fluxes as well as the interface and near-surface meteorological elements which are important in determining the surface layer energy transports. The simulation experiments were based on initial data obtained from observations made during February-March 1964 over the eastern part of the Arabian Sea.

The results demonstrate that the model simulated vertical profiles of temperature and wind are in general agreement with observed structure of the atmospheric boundary layer over Arabian Sea. Comparison with observations of sea surface temperature and near-surface wind and humidity shows that the model is capable of realistic simulations. The model results include the vertical profiles of eddy fluxes of sensible heat, moisture and momentum within the atmospheric boundary layer.

1. Introduction

A one-dimensional air-sea interaction model has been adopted to simulate the detailed time and space (vertical) structure of the atmospheric boundary layer over Arabian Sea during winter monsoon season. The model is mathematically and physically based on the Eulerian conservation equations for momentum, heat, water vapour, salinity and pollutants and is capable of examining the transport and diffusion processes in the planetary boundary layer. The principal processes parameterized are boundary layer turbulence in stratified conditions, mixing due to wind-generated waves on the interface and cloud dependent radiative heating throughout the layer. In this paper, a comparison between direct observations and the model simulated near-surface meteorological conditions with five day average input data for the period 28 February-3 March 1964 are presented. The model results include the eddy fluxes of sensible heat, water vapour and momentum within the atmospheric boundary layer.

2. The Model description

The model equation takes the form

$$\frac{\partial x_i}{\partial t} + \mathbf{V} \cdot \nabla X_i = \frac{\partial}{\partial z}\left[K_i\,(R_i, z)\,\frac{\partial x_i}{\partial z}\right] + A_i \quad (1)$$

Where **V** is the velocity vector, z is height, t is time, K_i is the eddy exchange coefficient for the dependent variables X_i and R_i is the Richardson number. The dependent variables X_i and associated source terms A_i are listed in Table 1.

The Eqn. (1) is non-linear through the dependence of vertical diffusion coefficients on Richardson number. The vertical diffusion coefficients are internally computed in the model as a function of vertical gradients of wind, humidity and temperature. For water sub-surface, the formulae for the Richardson number and vertical diffusion include mixing length variations due to the presence of mean turbulent wave at the interface.

TABLE 1

Index	Dependent variables	Source termes
1	Eastward velocity	Geostrophic wind/current
2	Northward velocity	Geostrophic wind/current
3	Temperature	Solar and infrared radiation, latent heating and cooling
4	Specific humidity	Evaporation, precipitation and condensation
5	Salinity	Evaporation, precipitation
6	Pollutants	—

TABLE 2

Condition	Input
Initial	Vertical profiles of dependent variables
Upper and lower boundary	Specification of dependent variables for the duration of the simulation
Gradients	Horizontal gradiants of the dependent variables
Clouds	Cloud levels and types as a function of time for the simulation period
Interface	Geostrophic winds and currents

Although the model in its most general form simulates on a three-dimensional grid configuration (X, Y, Z), for this study the numerical solutions of Eqn. (1) are computed on a one dimensional grid by exercising the options built into the model (the horizontal gradients of the dependent variables are specified rather than predicted). Weighted centered differences approximate the vertical derivatives for the unevenly-spaced vertical grid and the solution scheme is implicit in time. Upwind-differences approximate the horizontal spatial derivatives for the advection terms.

The radiative source terms are computed at each time step. Both solar and infrared use empirical equations to cover their respective parts of the spectrum. In addition to standard absorbers and scatterers, clouds and pollutants are included in the model.

A complete description of the model has been given elsewhere by Jacobs and Pandolfo (1974).

3. The Input data

The specific data requirements for the model simulation are listed in Table 2.

Our simulation experiment was based on input data collected during 28 February—3 March 1964 over the eastern part of the Arabian Sea. Data sources used in this study include a two volume set of International Indian Ocean Expedition Meteorological Atlas, Oceanographic Atlas of the IIOE, U.S. Navy Marine Climatic Atlas for Indian Ocean, Dutch Indian Ocean Oceanographic and Meteorological Data Collection and observations made by U.S. Weather Bureau and Woods Hole Oceanographic Institution research aircrafts and by oceanographic vessels in the eastern Arabian Sea during the phase II of the IIOE. Fig. 1 depicts the position of the buoy *Mentor* which recorded the wind, temperature and humidity in the lowest 8 metres of the atmospheric boundary layer while the dropsonde released from USWB and WHOI research aircrafts sampled the vertical profiles of pressure, temperature and humidity over the Arabian Sea.

A non-uniform grid system was used and the vertical layer extended from 400 metres below the air-water interface to 1500 metres above the surface. The grid levels used for the simulation are listed in Table 3.

The profiles of temperature, humidity/salinity and wind components were provided as initial conditions at all grid levels except at the upper and lower boundaries where the imposed boundary conditions required that the dependent variables be specified at each time step. In our simulation, these boundary conditions were specified as time-varying parameters. The data on the sea-current components at various depths were not available and, for our simulation, the lowest portion of the ocean was taken as being initially at rest. The horizontal gradients of the air temperature, wind and humidity were input to the model and remained constant throughout the simulation. The horizontal gradients of ocean temperature and salinity were calculated from a least square fit of a plane to three

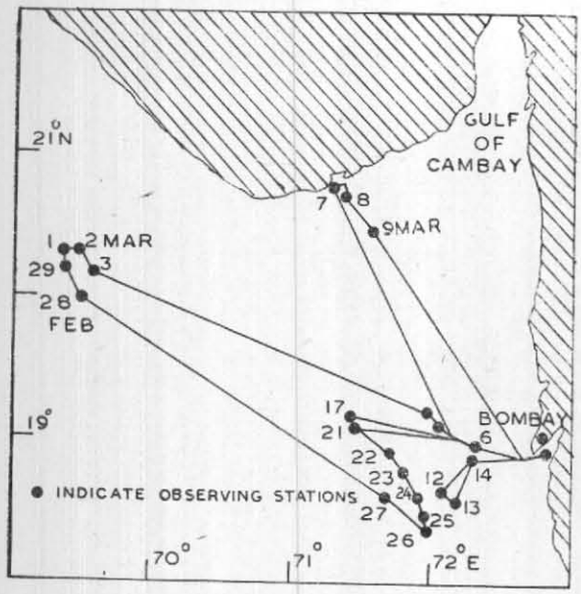

Fig. 1

TABLE 3

Height (depth) of vertical grid levels (m)
1500·0
1200·0
800·0
500·0
300·0
100·0
25·0
8·0
4·0
0·0
0·0
—0·25
—0·5
—1·0
—5·0
—10·0
—25·0
—100·0
—200·0
—400·0

average profiles in the eastern Arabian Sea. A time-varying cloud cover representative of the observed clouds in the region during the simulation period was input to the model. The initial time for the simulation was chosen to be 1200 hour (local time) of 28 February 1964 and a 96 hour simulation was carried out. The length of the time step was 4·8 minutes which made 75 time steps equal to 6 simulation hours.

4. Results

Three sets of comparisons between the model results and the actual observations are presented here. These sets are near surface meteorological elements, major components of interface heat budget and time-averaged vertical profiles of air temperature and wind speed. The time-averaged vertical profiles of model simulated stress and latent and sensible heat fluxes are also presented.

4.1. *Near surface meteorological elements*

The elements chosen for comparison are sea surface temperature and air temperature, humidity and wind at 8 metres above the air-water interface. Figs. 2(a) and 2(b) show the observed and model simulated sea surface temperature and air temperature at 8 m as a function of time. The most apparent characteristic of model simulated temperature is the diurnal variation. The simulated specific humidity at 8 m grid level is compared with observed specific humidity in Fig. 3. The model humidity remains slightly lower than observed values throughout the simulation period. The simulated wind speed and direction at 8 m show general agreement with actual observations shown in Figs. 4(a) and 4(b).

4.2. *Interface heat budget components*

Two major components of the interface heat budget in the tropical oceans are the rate of heat storage in the mixed oceanic layer Q_θ and the solar radition penetrating the sea surface Qs [$Q_S = (1-a)\, R_S$, where R_S is the incoming shortwave radiation and a is the albedo of the sea surface]. The term Q_θ is effectively the sensible heat transfer to the water if the flux of heat through the bottom of the mixed layer is negligibly small. Figs. 5(a) and 5(b) compare these observed heat budget components with model simulated results. The solar radiation penetrating the water surface Q_S is shown in Fig 5(a). The model results have been averaged over the duration of simulation period. Fig. 5(b) shows Q_θ calculated from the simulated average diurnal temperature change in the top 25 metres of water. The observed values of Q_θ were calculated from the five day average of the

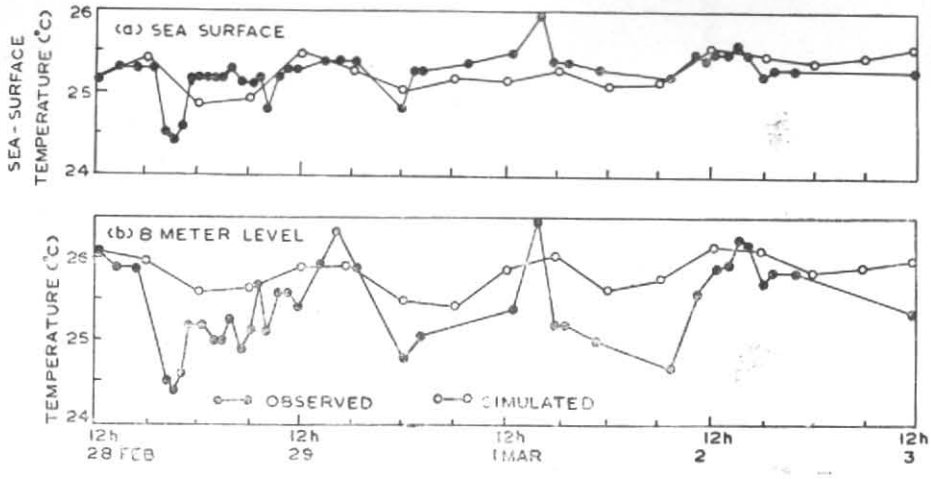

Fig. 2

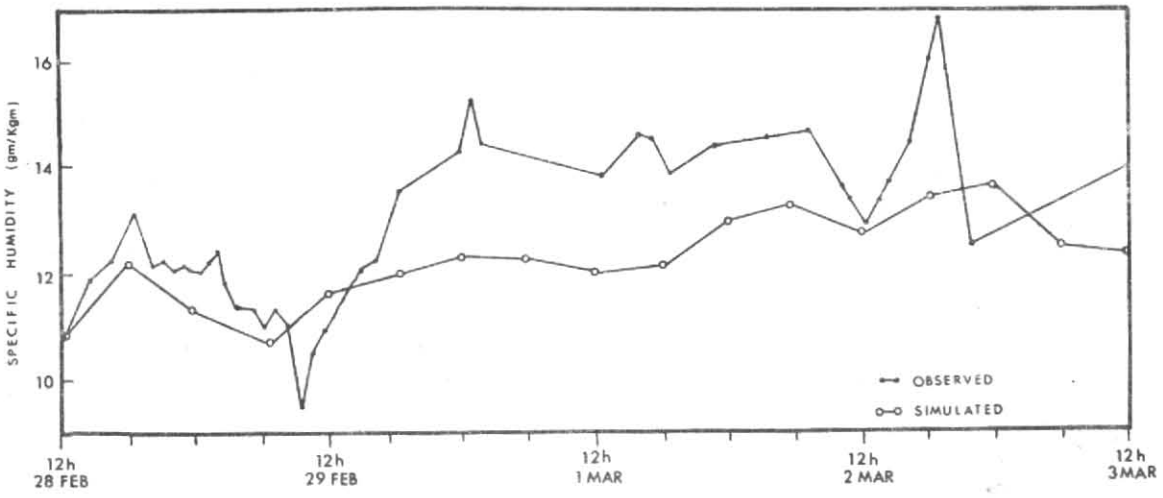

Fig. 3. The specific humidity at 8 metre level as a function of time

diurnally varying temperature profile. The set of averaged simulated temperature profile contains eight profiles daily at three hour intervals with average being taken over 96 simulation hours. Values obtained from both observed and simulated temperature profiles were plotted at the centre of the time interval over which temperature difference was taken.

4.3. *Vertical profiles*

In Figs. 6(a) and 6(b) time-averaged vertical profiles of temperature and wind speed from model simulation are compared with observed time-averaged vertical profiles. An average of air temperature over 96 simulation hours was taken to construct the model profile shown in Fig. 6(a). The observed profile was constructed from aircraft data and surface observations. The model temperatures are higher than the observed values in the lowest 300 metres above which simulated temperatures are lower than observed temperatures. The maximum discrepancy between simulated and observed temperatures occurs at 800 m and is of the order of 2°C. The comparison of vertical profiles for the horizontal wind speed is shown in Fig. 6(b). The simulated profile was constructed by time averaging of the eastward and northward components over the 96 hour simulation period. The observed profile consists of time averaged

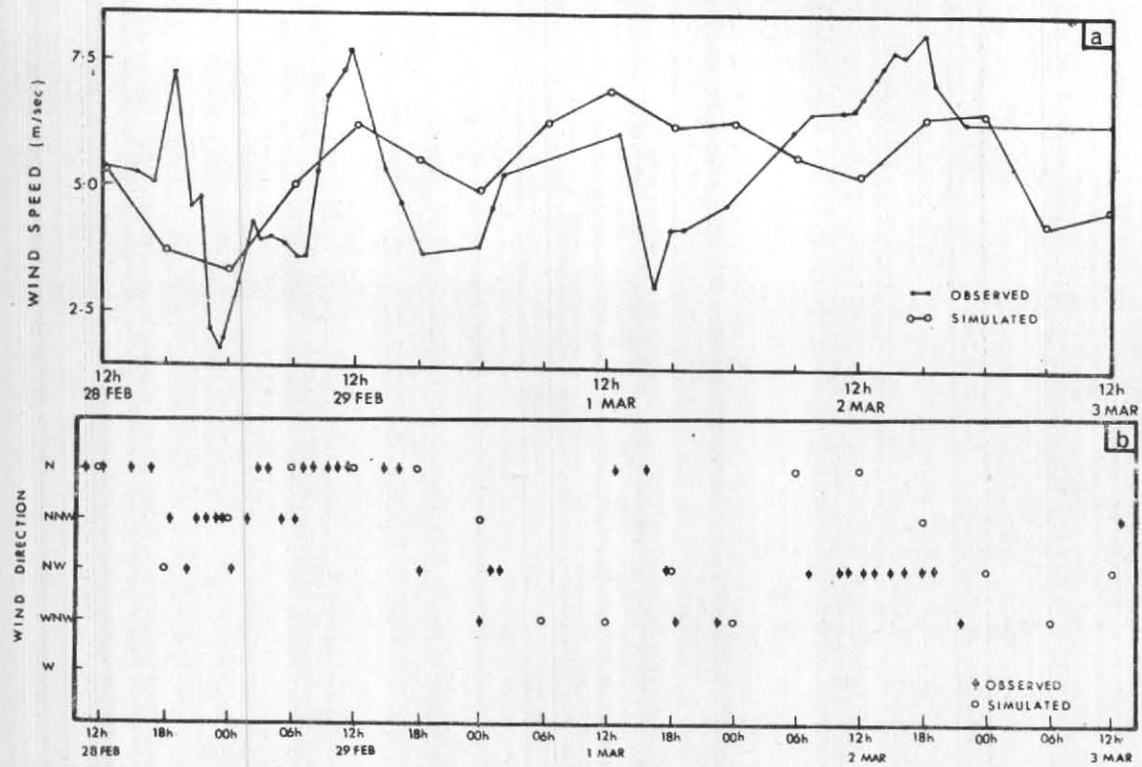

Figs. 4 (a-b). Comparison between model simulated and observed wind speed and direction at 8 m as a function of time

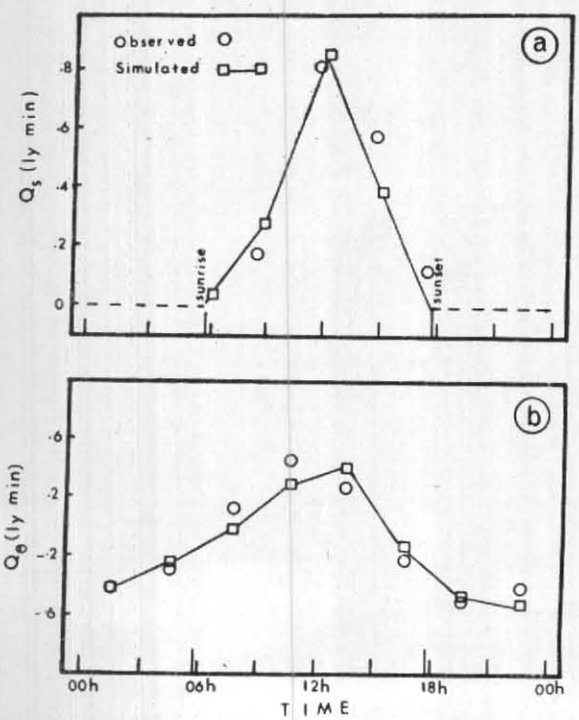

Fig. 5 (a). The average solar radiation penetrating the surface as a function of time

(b). The average rate of heat storage in the upper 25 m of water as a function of time

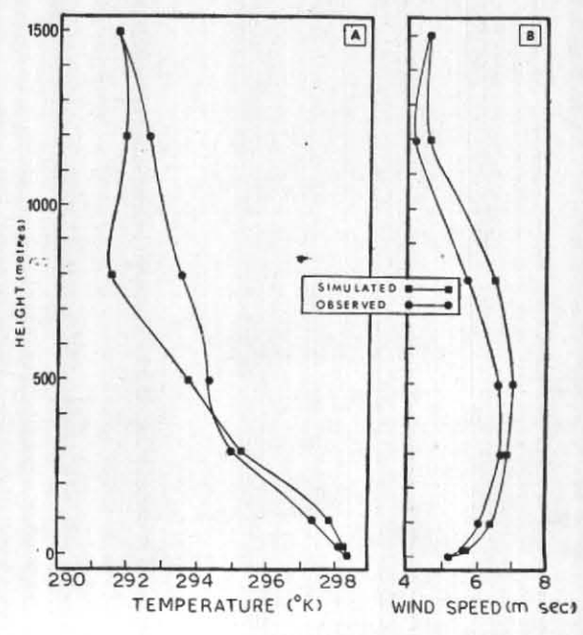

Fig. 6 (a) Fig. 6 (b)

Figs. 6 (a-b). A comparison of observed time-averaged vertical profiles of temperature and wind speed to those obtained by simulation

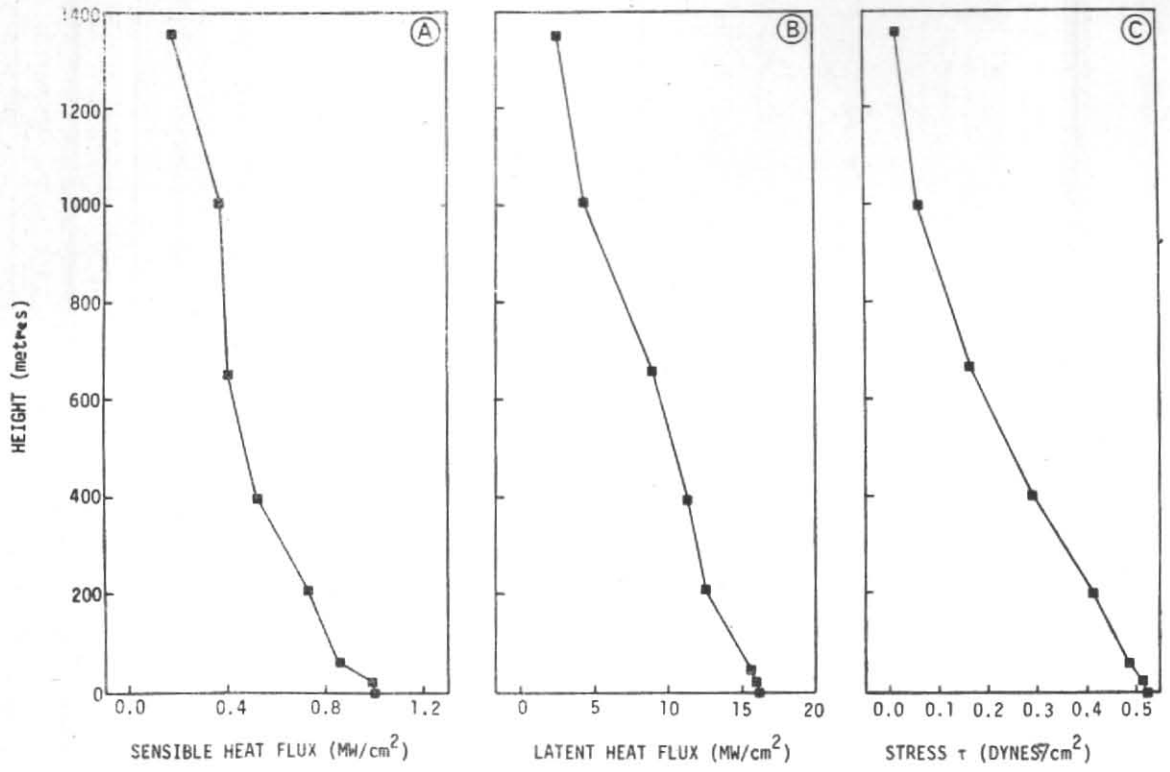

Fig. 7 (a) Fig. 7 (b) Fig. 7 (c)

Figs. 7 (a-c). The time averaged vertical profiles of eddy fluxes of sensible heat, moisture and momentum as obtained by the model simulation

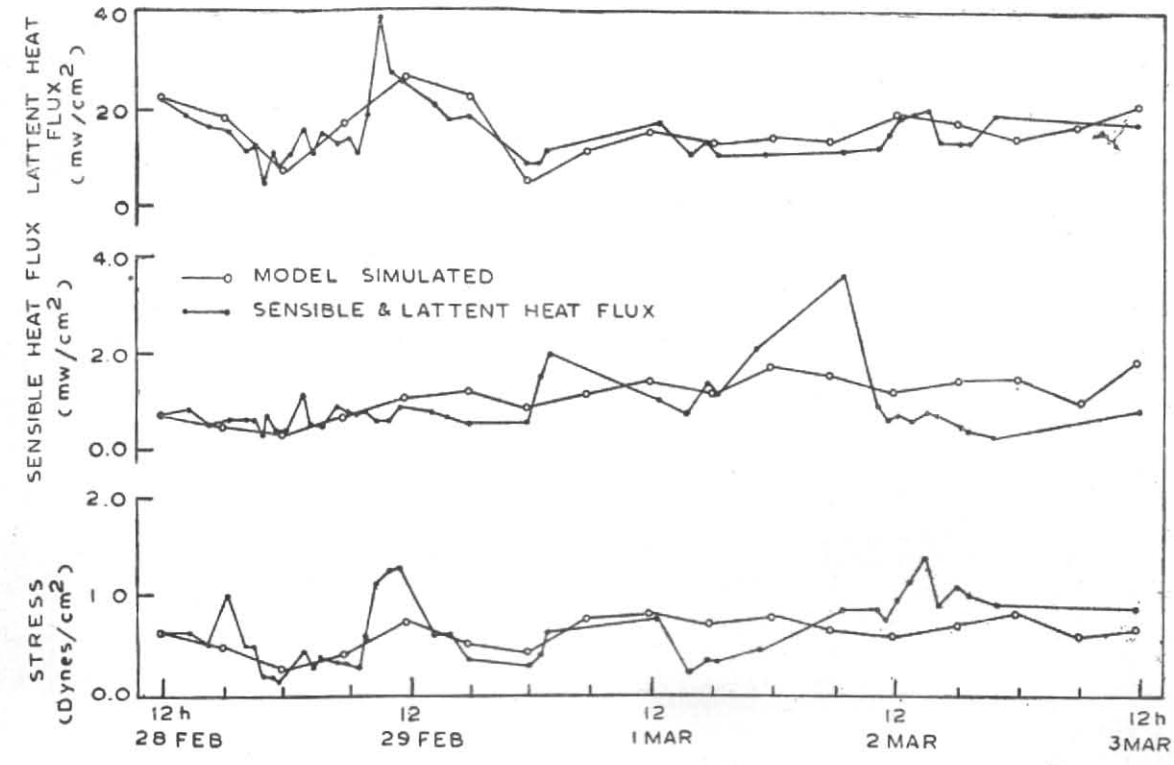

Fig. 8

TABLE 4

Bulk aerodynamic coefficients for Arabian Sea

Source	Drag coefficient C_D	Stanton number C_T	Dalton number C_q
Pond *et al.* (1974)	$(1{\cdot}55 \pm 0{\cdot}28) \times 10^{-3}$	$(1{\cdot}67 \pm 0{\cdot}69) \times 10^{-3}$	$(1{\cdot}42 \pm 0{\cdot}40) \times 10^{-3}$
Model simulation	$1{\cdot}40 \times 10^{-3}$	$1{\cdot}51 \times 10^{-3}$	$1{\cdot}51 \times 10^{-3}$

surface and upper wind observations collected on board the ship *Ocean*. The simulated wind speeds are consistently higher than the observed values throughout the profile.

The vertical profiles of model simulated turbulent fluxes have been time averaged for the duration of the simulation and are presented in Figs. 7(a), 7(b) and 7(c). In all three cases, the simulated fluxes decrease with height and not much of a vertical variation is observed. It may be mentioned here that, unlike these time averaged profiles, the individual simulated profiles of turbulent fluxes exhibited a diurnal variation with intermediate maxima and minima during the course of a day. The maximum value of this variation occurred at about 800 metres.

The model results of near surface stress and sensible and latent heat fluxes are compared to those reported by Badgley *et al.* (1972) in Fig. 8. A comparison of non-dimensional turbulent transfer coefficients reported by Pond *et al.* (1974) and those yielded by the model simulation for Arabian Sea is presented in Table 4.

5. Summary and Conclusion

The model, given appropriate input data, has succeeded in reproducing the near-surface atmospheric conditions over the Arabian Sea. The maximum departure between simulated and the observed interface temperature is of the order of 1·5°C. The simulated low-level humidity is slightly lower than the observed values almost throughout the simulation period. The simulated near-surface wind speed is somewhat higher than the observed wind but the model captures the prevalent direction. Verification of two major interface heat budget components shows that the model realistically simulates the diurnal variation of radiation penetrating the sea surface and also the rate of change of heat storage in the oceanic mixed layer. The time-averaged vertical profiles of temperature and wind speed simulated by the model are close to the observed profiles except that the temperature at about 800 m has been underestimated by about 2°K. The model generated vertical profiles of eddy fluxes of momentum and latent and sensible heat are in general agreement with aircraft based measurements.

The results demonstrate that the model is capable of realistic simulations of vertical structure of the atmospheric boundary layer over the Arabian Sea during the NE monsoon season. While experiments are being planned for the one-dimensional simulation of boundary layer over Arabian Sea during SW monsoon, at the moment, lack of required data prevents the simulation on a three-dimensional field. It is hoped that, during the forthcoming monsoon experiments, the systematic collection of data over the Indian Ocean would enable us to test the generalized three-dimensional model for the numerical simulation of the temporal and spatial structure of the boundary layer over Arabian Sea.

Acknowledgements

This study was financially supported by the National Research Council of Canada which is gratefully acknowledged. Essential data were supplied by National Oceanographic Data Center (NOAA), Woods Hole Oceanographic Institution, Indian Institute of Tropical Meteorology and National Climatic Data Center (Asheville). The typing of the manuscript by Mrs. June Hawkins is appreciated.

REFERENCES

Badgley, F. I., Paulson, C. A. and Miyake, M.	1972	Profiles of wind, temperature and humidity over Arabian Sea, IIOE Met. Monogr., **6**, 62. pp.
Jacobs, C. A. and Pandolfo, J. P.	1974	A description of a general three-dimensional numerical simulation model of a coupled air-water and/or air-land boundary layer, CEM Report No. 4131-509a., 1., 85 pp.
Pond, S., Fissel, D. B. and Paulson, C. A.	1974	A note on bulk aerodynamic coefficients for sensible heat and moisture fluxes, *Boundary Layer Meteorology*, **6**, pp. 333-339.

DISCUSSION

C. RANGARAJAN : Did you find a diurnal variation in vertical diffusivity over the Arabian Sea ?

AUTHOR : Yes, I did.